Seasonally distinct sources of N_2O in acid organic soil drained for agriculture as revealed by N_2O isotopomer analysis

Søren O. Petersen · Reinhard Well · Arezoo Taghizadeh-Toosi · Tim J. Clough

Abstract Acid organic soils drained for agriculture are hotspots for nitrous oxide (N_2O) emissions. Previous studies have indicated that water table (WT) depth and nitrogen (N) availability are important environmental controls, however, little is known about pathways leading to N_2O emission. We investigated a raised bog drained for agriculture (pH 4.6 to 5.5) with, respectively, rotational grass and a potato crop in the experimental year and subplots with and without N fertilisation. The emissions and isotopic composition of N_2O were monitored during spring and autumn periods with significant changes in WT depth, and in the availability of ammonium (NH_4^+) and nitrate (NO_3^-). Nitrous oxide emissions were determined at 6-h intervals using eight automated chambers interfaced with a laser instrument for N_2O isotopomer analysis. A threshold of 600 ppb N_2O (final concentration) was adopted to stabilise estimates of site preference (SP) and $\delta^{15}N_{bulk}$ of emitted N_2O against the background of N_2O in ambient air. Nitrous oxide emissions varied consistently with land use, slope position and time of day and year, but with little effect of N fertilisation. Isotopic signatures of N_2O from the grassland site could not be investigated due to generally low emissions. In the potato field, in total 255 and 266 flux measurements exceeded the 600 ppb threshold in unfertilised and fertilised subplots, respectively. Both N_2O emissions and isotopic signatures responded to WT dynamics, individual rain events, and soil N availability. Across eight individual periods, the $\delta^{15}N_{bulk}$ of N_2O emitted from the soil varied between -55 and $+18‰$, while site preference (SP) varied between -4 and $+25‰$. The first and the last period (shoulder seasons) were both N limited, and here isotopic signatures of N_2O were similar and distinctly different from signatures in mid-season periods with mineral N accumulation. Nitrifier denitrification and chemodenitrification were proposed as potential pathways to N_2O production in shoulder seasons, whereas in mid-season periods the isotopic signatures could be associated with either ammonia oxidation or fungal denitrication (late spring), or with bacterial denitrification (early autumn). The interpretation of isotopic signatures of N_2O was confounded by the possible effect of N_2O

S. O. Petersen (✉) · A. Taghizadeh-Toosi
Department of Agroecology, Aarhus University, Blichers allé 20, 8830 Tjele, Denmark
e-mail: sop@agro.au.dk

R. Well
Thünen Institute of Climate-Smart Agriculture, Bundesallee 65, 38116 Braunschweig, Germany

T. J. Clough
Faculty of Agriculture and Life Science, Lincoln University, Lincoln 85084, Canterbury, New Zealand

reduction. The study provides evidence that both sources and pathways of N_2O emissions from managed organic soil vary dynamically with WT changes and N availability.

Introduction

Drainage of organic soils (Histosols) for cultivation accelerates decomposition of the peat layer, resulting in subsidence and net release of the radiatively active gases CO_2 and N_2O (Mander et al. 2010). Nitrous oxide emissions from organic soils are classified according to land use and nutrient status (IPCC 2014). However, soil physical and chemical properties (Leppelt et al. 2014), groundwater dynamics (Aerts and Ludwig 1997; Goldberg et al. 2010), and field operations such as fertilisation and vegetation cover during the year (Leppelt et al. 2014), have interacting effects on soil N transformations, which result in seasonal variation in N_2O emissions (Taghizadeh-Toosi et al. 2019).

There are several possible pathways to N_2O formation in partly drained organic soils, which may involve biotic, as well as abiotic, processes occurring under aerobic or anaerobic conditions. Biotic pathways under aerobic conditions include ammonia oxidation by archaea or bacteria (Herrmann et al. 2012; Stieglmeier et al. 2014), and with O_2 limitation pathways may include nitrifier denitrification, as well as bacterial and fungal denitrification (Liu et al. 2014). Abiotic formation of N_2O can occur through chemodenitrification (Van Cleemput and Samater 1996). Biotic codenitrification has also been described, but this process is restricted to neutral pH (Spott et al. 2011). Molecular characterisation of microbial communities and their activity can help identify potential pathways (Andert et al. 2011; Herrmann et al. 2012; Görres et al. 2013), but linking emissions with specific populations in a variable soil environment is difficult. In this study, N_2O isotope analyses were used instead in an attempt to identify biotic or abiotic drivers of N_2O emissions from managed organic soils.

The isotopic signature of N_2O produced under conditions without substrate limitation carries information about its origin (e.g., Sutka et al. 2006; Toyoda et al. 2017). The predominant form of N_2O in atmospheric air is $^{14}N^{14}N^{16}O$, but each of the N atoms may be substituted with ^{15}N to form two other isotopocules of N_2O, i.e., $^{15}N^{14}N^{16}O$ and $^{14}N^{15}N^{16}O$, which are isotopic isomers, or isotopomers, of N_2O. For a discussion of the terminology, see Toyoda et al. (2013). The isotopologue ratios $^{14}N^{15}N^{16}O/^{14}N^{14}N^{16}O$ ($^{15}R^{\alpha}$) and $^{15}N^{14}N^{16}O/^{14}N^{14}N^{16}O$ ($^{15}R^{\beta}$) are typically expressed relative to air-N_2 as:

$$\delta^{15}N^{\alpha} = \left[{}^{15}R^{\alpha}_{sample} \Big/ {}^{15}R^{\alpha}_{air} - 1 \right] \times 1000 \qquad (1)$$

$$\delta^{15}N^{\beta} = \left[{}^{15}R^{\beta}_{sample} \Big/ {}^{15}R^{\beta}_{air} - 1 \right] \times 1000 \qquad (2)$$

$$\delta^{15}N^{bulk} = \left[{}^{15}R^{bulk}_{sample} \Big/ {}^{15}R_{air} - 1 \right] \times 1000$$
$$= (\delta^{15}N^{\alpha} + \delta^{15}N^{\beta})/2 \qquad (3)$$

The difference in ^{15}N enrichment between the central and terminal positions of N in the N_2O molecule, termed the *site preference* (SP), is defined as: SP $= \delta^{15}N^{\alpha} - \delta^{15}N^{\beta}$ (Toyoda 2013). Since individual N_2O production pathways have characteristic signatures with respect to SP and $\delta^{15}N_{bulk}$ of N_2O, the isotopic signature of N_2O emitted from soil may also hold information about source composition (Park et al. 2011; Hu et al. 2015; Toyoda et al. 2017).

To determine isotope ratios of N_2O emitted from soil, pre-concentration is necessary (Mohn et al. 2012; Toyoda et al. 2017). For measurements in open air, a separate pre-concentration unit has been developed (Mohn et al. 2010; Wolf et al. 2015), but if non-steady state chambers are used for soil-air flux measurements, then N_2O accumulating within the chamber headspace provides "pre-concentration" during chamber deployment.

This study was part of a monitoring program investigating N_2O emissions from an acid peat soil during spring and autumn periods (Taghizadeh-Toosi et al. 2019). We expected that N_2O emission patterns would be dominated by the effects of vegetation cover and N fertilisation, as modified by climate (Leppelt et al. 2014). Based on previous observations at this site (Petersen et al. 2012), we specifically hypothesized that N_2O emissions from the arable site with potato cropping would be higher than from grassland, and that high N_2O emissions would be associated with water table (WT) decline in spring, and with WT rise

in the autumn. We further hypothesized that N_2O isotopic composition could be determined at sufficient precision to investigate pathways of N_2O formation.

Materials and methods

Site description

The study took place within a raised bog in Northern Denmark, in an area drained for agriculture. The shallow peat had a depth of 60 to 90 cm, and pH in the soil profile varied between 4.6 and 5.5. The area has previously been characterised as potentially acid sulfate soil (Madsen and Jensen 1988), but iron sulfide concentrations were low compared to concentrations of total reactive iron, comprising ferrous iron and reducible ferric iron (Taghizadeh-Toosi et al. 2019), and thus reactive iron in the raised bog was probably dominated by iron oxides/hydroxides (Madsen et al. 2000). The site was characterised by considerable seasonal variation in groundwater level (Petersen et al. 2012), and WT depth varied between 20 and 90 cm during the periods investigated in this study. Soil profiles were sampled to 1 m depth for determination of total N and $\delta^{15}N$ in June 2015 (DOY166); 5 cm sections from selected depths were dried and ball-milled, and analysed at the UC Davis Stable Isotope Facility using a PDZ Europa ANCA-GSL elemental analyzer interfaced to a PDZ Europa 20-20 isotope ratio mass spectrometer (Sercon Ltd., Cheshire, UK).

The two sites investigated were located side by side in neighbouring fields with, respectively, rotational grass and a potato crop in 2015. These sites and crops were also included in the monitoring study of Petersen et al. (2012), where they were referred to as sites *N-RG* and *N-AR*, respectively. Weekly N_2O emissions and associated soil conditions during spring and autumn were reported for these two sites by Taghizadeh-Toosi et al. (2019), and in line with the notation used in that study, the two sites will be referred to as *AR1* (arable site) and *RG1* (rotational grass), respectively.

At each site, a 10 m × 24 m area was fenced and subdivided into three blocks of 8 m × 10 m, each with a centrally positioned piezometer tube (Rotek A/S, Sdr. Felding, Denmark) installed to 150 cm depth for monitoring of WT depth (Fig. 1). The site had a small slope in a north–south direction, corresponding to a difference in WT depth of *c.* 15 cm between block

1 and 3. Each site was further subdivided along its longitudinal axis to establish two 5 m × 24 m sub-plots, one of which received N fertiliser according to the rate given outside the fenced area, whereas the other subplot received no N fertiliser. Air temperature, wind speed, barometric pressure and relative humidity were recorded as hourly averages using a Kestrel 4500 mobile weather station (Nielsen-Kellerman; Booth-wyn, PA). Hourly precipitation and some temperature data, lost due to a technical error, were obtained from a meteorological station 8 km from the sites.

Except for N fertilisation, management within the fenced areas (tillage, seeding, cuts and harvest) followed management of each field; fencing and equipment were removed and reinstalled as required. The fertilised $(+ F)$ subplot of *RG1* received 350 kg ha^{-1} NS 27-4 as pelleted fertiliser on 16 April (DOY106), which corresponded to 94.5 kg N ha^{-1}. The fertilised part of site *AR1* received 100 kg N ha^{-1} as liquid NPS 20-3-3 fertiliser on 21 May (DOY141). The NS fertiliser contained equal amounts of ammonium (NH_4^+) and nitrate (NO_3^-), while the NPS fertiliser contained mainly NH_4^+. The field of site *RG1* was grazed by heifers outside the fenced area; inside the fence the grass was instead cut in late August (around DOY245). Potato harvest at site *AR1* took place in mid-September, but the harvest (and consequently the measurements) were interrupted for more than a week due to extensive rainfall.

Analytical setup

The setup for flux measurements consisted of a LI-8100A automated soil gas flux system (LI-COR Ltd., Cambridge, UK) with eight chambers (20 cm diameter sampling area) and a LI-8150 multiplexer. Extension cables to auto-chambers were 15 m long, and chambers CH1 to CH8 were positioned in block 2 and 3 as shown in Fig. 1. Hence, there were two sampling positions in each land use and fertiliser treatment. A N_2O Isotope Analyzer (Part No. 914-0022-0000; Los Gatos Research, Mountain View, CA) was connected in parallel to the LI-COR system as recommended by Li-Cor Ltd. (LI-COR 2014). The inlet for the laser instrument was connected to the outlet from the LI-8100A analytical unit, and returned before the inlet for the LI-8150 multiplexer (Fig. 2). To allow for analysis of reference gases, the interface included a six-port valve fitted with a microelectric
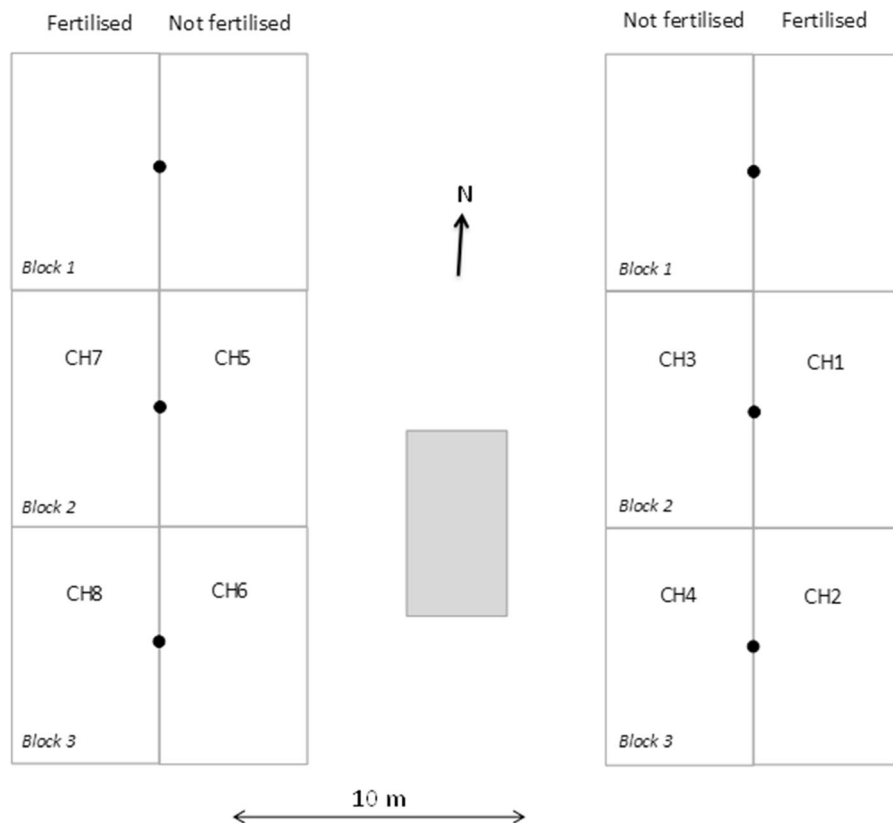
Fig. 1 Design of the experimental sites AR1 (left) and RG1 (right). Positions of auto-chambers CH1-CH8 are indicated. The shaded area represents the trailer with analytical equipment.

Fertilised ($+ F$) and unfertilized ($- F$) subplots (5 m × 24 m) are indicated; for details regarding fertilisation, see text

actuator (Model ET4VL6MWE2; VICI Valco Instruments Co. Inc.) and separate multiplexer for the laser system (Part No. 908-0003-9002). In the 'analysis position', the internal pump of the laser instrument sampled from the LI-8100 outlet at approx. 100 ml min^{-1}, much less than the recirculating flow of the LI-8100A system of c. 3 l min^{-1}. In the 'flush position', there was no active flow through the parallel gas line, while the laser instrument analysed reference gas or ambient air.

All gas sampling lines were equipped with a 1 μm in-line disk filter to remove particles, but traps for water or CO_2 were not used. According to the manual, N_2O concentrations and isotope ratios are corrected for water vapour, and in accordance with this a post hoc analysis of a subset of data ($n = 33$) with final relative humidity (RH) ranging from 37 to 95% did not show significant effects of RH on $\delta^{15}N_{bulk}$ ($r^2 = 0.02$, $p = 0.51$) or SP ($r^2 = 0.005$, $p = 0.14$). Nitrous oxide isotope ratios determined by laser spectroscopy are

sensitive to CO_2 concentration, and Erler et al. (2015) described a near linear decline with increasing CO_2 between 0 and 10,000 ppm using a Picarro G5101-I instrument. A comparable interference was observed with the instrument used in the present study, where $\delta^{15}N_{bulk}$ changed by $- 3.1$‰ in a mixture of 2000 ppb N_2O and 2000 ppm CO_2. However, the overall maximum increase in headspace CO_2 concentration during chamber closure was 365 ppm, which corresponded to maximum errors due to CO_2 of $- 0.6$‰.

Chambers were operated with the LI-8100A system software, but data were collected from both instruments with a separate program, developed for this setup by CIM Industrial Systems A/S (Hasselager, Denmark), which also recorded multiplexer port positions and chamber status (open, closed). Measurements by the LI-8100A system were not used, except that the recorded relative humidity was used in the evaluation of N_2O isotope data. The chamber closure time had to be balanced against the need for N_2O
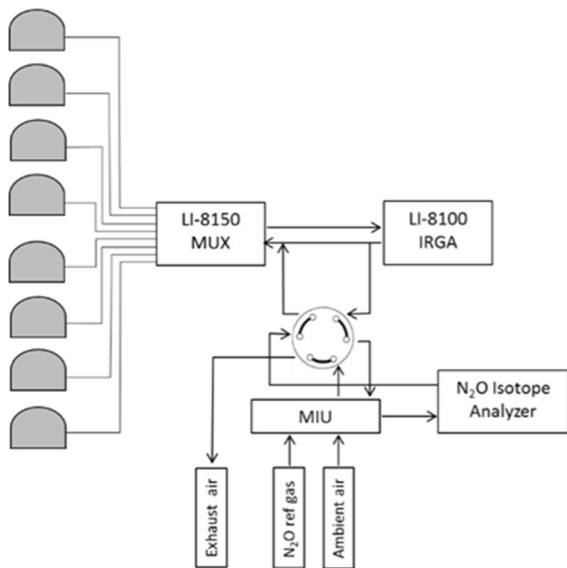
Fig. 2 A diagram showing the configuration of the experimental setup for monitoring isotopomer composition and flux of N_2O with eight automated chambers. MUX is the multiplexer of the LI-COR system, and MIU the multiport inlet unit of the laser instrument

concentrations and isotope ratios to return to ambient levels between the individual flux measurements, and allowing also for analysis of reference gases between cycles. The sampling routine included a cycle of flux measurements from the eight chambers every 6 h, where the chamber closure time was 12 min and flushing time between flux measurements 18 min. Thus, flux measurements were conducted at 30 min intervals within each cycle. Between measurement cycles, ambient air and a 2008 ppb N_2O reference gas (Air Products NV; Diegem, Belgium) were analysed in triplicate for 12 min periods. However, due to delays in the software development, the automated analysis of reference gases only became available during the autumn measurement campaign, and hence during spring the calibration relied on data obtained manually during field trips.

The laser instrument and LI-COR analytical unit, multiplexers and N_2O reference gases were placed in an insulated trailer equipped with an Acson inverter (Ahlsell; Brøndby, Denmark) for climate control. Instruments were operated from a laptop with remote access via a D-Link 108G wireless router, and the N_2O Isotope Analyser through a VNC connection from the laptop.

Spring and autumn measurement campaigns

The collars for automated chamber sampling positions were installed to between 3 and 5 cm depth and the average extension of each collar recorded. Flux measurements were initiated on 22 March 2015 (DOY81). Interrupted only by field operations for establishment of the potato crop at site *AR1*, monitoring continued until 14 June (DOY165). As stated above, four cycles of measurements were completed in each 24-h period. Measurements alternated between auto-chamber positions at the *RG1* and *AR1* sites in the following order: CH1, CH5, CH2, CH6, CH3, CH7, CH4 and CH8 (cf. Fig. 1).

In the autumn, the monitoring program was resumed on 2 September (DOY245), but due to technical problems with power failure, and then delays in the potato harvest due to extensive rainfall, only results from a 48-h period (DOY258-260) were obtained until DOY268. Measurements then continued until early November, but from 1 October (DOY274) the N_2O flux rates dropped to a level where the N_2O isotopic composition (see below) could only be determined for a few fluxes, and these results are therefore not considered further.

Soil samples ($n = 6$) were taken weekly to 50 cm depth in each subplot ($AR1 + F$, $AR1 - F$, $RG1 + F$ and $RG1 - F$), and soil from the 0 to 25 cm and the 25 to 50 cm depth intervals pooled. Ten-gram subsamples were extracted in 1 *M* KCl and filtered; the filtrates were analysed for NH_4^+–N and $(NO_2^- + NO_3^-)$–N, henceforth NO_x^-, by standard colorimetric methods.

In June 2015 (DOY166), intact cores were taken to *c.* 100 cm depth near sampling positions in block 2 of *RG* and *AR* sites using a stainless steel corer (04.15 SA/SB liner sampler, Eijkelkamp, Giesbeek, Netherlands) with a plastic sleeve (diameter: 5 cm, length: 30 cm).

Data analysis

Soil $\delta^{15}N$ and total N concentration at 0 to 5, 5 to 10, 15 to 20, 45 to 50 and approximately 95 to 100 cm depth intervals in $+ F$ and $- F$ subplots of sites *RG1* and *AR1* were compared with separate two-way ANOVA tests.

Nitrous oxide fluxes were calculated using the software package HMR for R (R Core Team 2016) as

described by Pedersen et al. (2010). The 12-min concentration–time series showed a mixture of linear and curvilinear developments in N_2O accumulation. The proportion of curvilinear fluxes estimated using HMR ranged from 44 to 87%, but there was no evidence for systematic effects of land use or rainfall on curvilinearity (data not shown).

The repeatability of isotope ratio measurements was evaluated for Period IV (described below) by calculating standard deviations of the triplicate analyses of a 2008 ppb N_2O reference gas analysed between cycles of chamber measurements; for this period the standard deviations averaged 0.32‰ (range 0.01–0.71‰) for SP, and 0.21‰ (range 0.01–0.40‰) for $\delta^{15}N_{bulk}$ of N_2O ($n = 22$). As indicated above, interference from CO_2 was an additional source of variability between sampling positions of up to 0.6‰, increasing the potential uncertainty of $\delta^{15}N_{bulk}$ of N_2O to around 1‰. Nitrous oxide concentrations were recorded at 0.1 Hz (Fig. 3a, d). At this data collection rate, the Allan variance of $\delta^{15}N_{bulk}$ in ambient air, i.e., the variance of differences between adjacent 10 s intervals, was 1–2‰ (Fig. S1). However, since SP and $\delta^{15}N_{bulk}$ were calculated for N_2O in excess of ambient air, the precision for soil-derived N_2O was much

poorer and declining as N_2O concentrations declined. In order to stabilise estimates, we calculated running means and standard deviations for both SP and $\delta^{15}N_{bulk}$ representing a 100 s time window. These time-averaged values of SP (Fig. 3b, e) and $\delta^{15}N_{bulk}$ of emitted N_2O (Fig. 3c, f) were still highly variable at low mixing ratios, but stabilised as concentrations of N_2O in excess of the atmospheric background increased. On the basis of scatter plots of standard deviations of SP and $\delta^{15}N_{bulk}$ as a function of N_2O concentration (Fig. S2, spring only), a threshold of 600 ppb N_2O (final concentration) was selected for calculation of SP and $\delta^{15}N_{bulk}$. Here, the standard deviation of SP and $\delta^{15}N_{bulk}$ of N_2O were up to around 20 and 10‰, respectively.

Due to the 600 ppb N_2O final concentration threshold used, very few observations (< 20 in total) of $\delta^{15}N_{bulk}$ and SP of N_2O were available from the rotational grass site (RG1). Therefore, for site RG1, only fluxes of N_2O will be presented, and not isotopic signatures. At site AR1 with a potato crop during the 2015 growing season, in total 804 fluxes were processed for analysis of isotopic signatures. Of these, 521 fluxes (65%) met the 600 ppb criterion, with 255
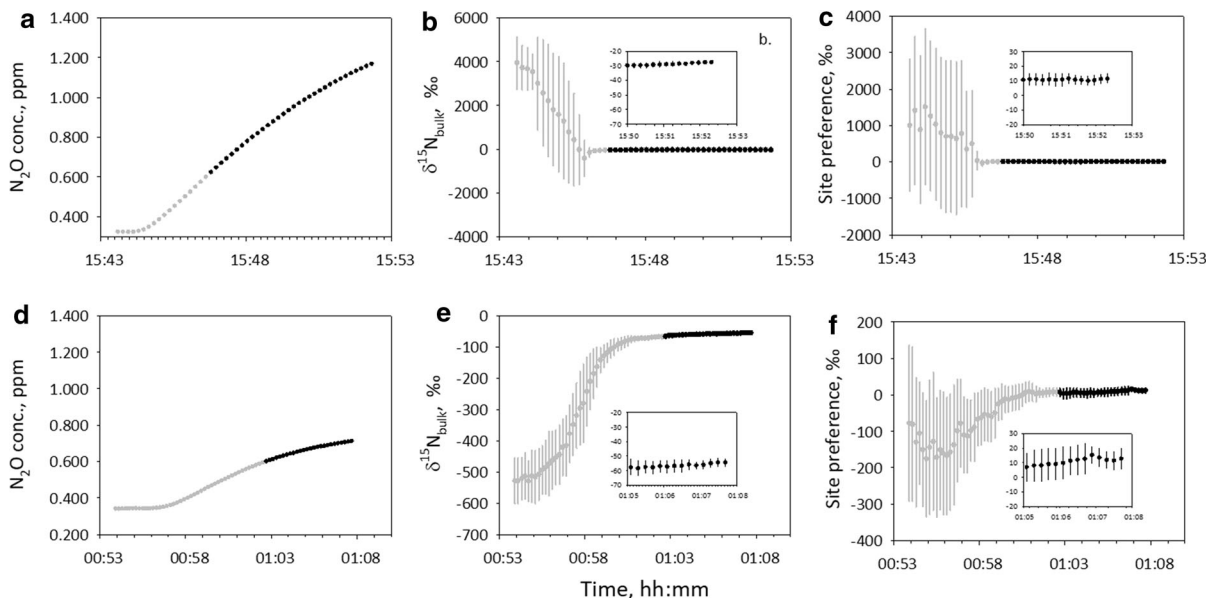
Fig. 3 Example data for flux measurements obtained on 10 April 2015 at position CH7 (top panel), and on 12 June 2015 at sampling position CH8 (bottom panel), with indication of the range of values (black) acceptable for analysis of isotopic signatures. Subplots a, d N_2O concentrations recorded at 0.1 Hz. Subplots b, e $\delta^{15}N_{bulk}$ of soil-emitted N_2O. Subplots c, f Site preference (SP) of soil-emitted N_2O. The results for SP and $\delta^{15}N_{bulk}$ represent running means and standard deviations of 10 consecutive measurements

and 266 flux measurements in unfertilised ($-\,F$) and fertilised ($+\,F$) subplots, respectively.

Correction of $\delta^{15}N^{\alpha}$ and $\delta^{15}N^{\beta}$ of N_2O was performed based on the 2008 ppb N_2O reference gas, for which $\delta^{15}N_{bulk}$, $\delta^{15}N^{\alpha}$ and $\delta^{15}N^{\beta}$ vs. N_2 in atmospheric air were $-\,0.5 \pm 0.07$, $-\,1.2 \pm 0.14$ and 0.2 ± 0.18‰ as determined by the isotope ratio mass spectrometry method described by Nguyen et al. (2017). The $\delta^{15}N_{bulk}$ and SP of N_2O were further corrected for concentration dependency in the range of 600–2000 ppb N_2O (Fig. S3). The SP and $\delta^{15}N_{bulk}$ of emitted N_2O were then calculated using a two-component mixing model (Well et al. 2006):

$$SP_{soil} = \frac{(SP_{mix} \times N_2O_{mix} - SP_{air} \times N_2O_{air})}{N_2O_{mix} - N_2O_{air}} \quad (4)$$

$$^{15}N_{soil}^{bulk} = \frac{\left(^{15}N_{mix}^{bulk} \times N_2O_{mix} - ^{15}N_{air}^{bulk} \times N_2O_{air}\right)}{N_2O_{mix} - N_2O_{air}}$$
$$(5)$$

where indices 'soil', 'air' and 'mix' refer to N_2O emitted from soil, N_2O in ambient air, and the mixture of these two pools, respectively.

The $\delta^{15}N_{bulk}$ and SP of N_2O emitted in eight individual periods were tested in R with the non-parametric Kruskal–Wallis analysis of variance followed by Dunn's multiple comparison test.

Results and discussion

Isotopic signature of soil and input

The $\delta^{15}N$ and total N of soil profiles at sites *RG1* and *AR1* are shown in Table 1. There were no significant differences in $\delta^{15}N$ between layers dominated by peat, with values ranging from $+\,2$ to $+\,4$‰. For comparison, Broder et al. (2012) found $\delta^{15}N$ values of $-\,3$ to $+\,3$‰ in soil profiles of three pristine bog peats. The higher values observed at 95–100 cm were associated with very low concentrations of total N, and are thus highly uncertain, although it may be noted that Gregory et al. (2016) reported an increase in $\delta^{15}N$ in profiles of a silty clay loam soil to around $+\,8$‰ at 75 cm depth, which is consistent with the values reported here.

There was no effect of fertilisation on soil $\delta^{15}N$ (Tables 1, 2). The pelleted NS fertiliser used at site *RG1* had a $\delta^{15}N$ of $-\,0.17 \pm 0.02$‰ ($n = 4$). Nishida and Sato (2015) reported that $\delta^{15}N$ of four synthetic

fertilisers, including ammonium sulfate and three compound fertilisers with N, P and K, were all in the range of $-\,2.5$ to 0‰. The $\delta^{15}N$ of potato crop residues was not determined, but Camin et al. (2007) reported that $\delta^{15}N$ of potato tubers grown at four sites ranged from $+\,2.2$ to $+\,4.1$‰. Given the narrow $\delta^{15}N$ range of peat, crop residues and fertiliser N, which are the potential sources of N_2O–N, significant deviations from the 0 to $+\,5$‰ range with respect to $\delta^{15}N_{bulk}$ of N_2O would thus be a result of soil N transformations.

Soil conditions

Water table dynamics are shown in Fig. 4. Unfortunately, during spring only weekly recordings were possible, but the autumn data show that WT depth changed dynamically after rainfall. In Fig. 4, four periods are indicated with declining or increasing WT depth during spring and autumn, respectively, for which detailed measurement results are presented below. These trends in WT changes were supported by permutation tests respecting the block structure (Taghizadeh-Toosi et al. 2019), except that the WT increase between DOY145 and 155 was not significant in the analysis of observations in spring ($p = 0.12$). Results from four other periods during spring are included as online Supplementary Information (Figs. S4 to S7), but not presented in detail.

Concentrations of NH_4^+ and NO_x^- at sites *RG1* (grass) and *AR1* (potato) during the spring and autumn monitoring periods are shown in Fig. 5. The standard errors are not shown, but coefficients of variation were typically 5–15% except immediately after fertilisation. At the grassland site, both NH_4^+ and NO_x^- were always close to the background level except for a 2-week period after fertilisation. At the arable site, there was also little mineral N in the soil until around DOY111, but then accumulation of both NH_4^+ and NO_x^- occurred, presumably as a result of peat N mineralisation. The transient decline shortly before N fertilisation on DOY141 followed 12 mm of rainfall on DOY139 (Fig. S6). There was a significant increase in NO_x^- concentrations, especially in treatment *AR1* $+\,F$, during May and June (DOY112-166), indicating that nitrification activity was high. The proportions of NO_2^- and NO_3^- were not determined regularly, but intact soil profiles collected to 1 m depth on DOY118 contained up to 10 mg NO_2^-–N kg^{-1} (Taghizadeh-Toosi et al. 2019).

Table 1 The ^{15}N enrichment and concentration of nitrogen in soil profiles collected at site AR1 and RG1 in June 2015 (DOY166)

Land use	Depth (cm)	δ^{15}N (‰)		Total N (%)	
		Avg.	S.E.	Avg.	S.E.
Rotational grass, RG1	0–5	3.53	0.71	1.76	0.10
	5–10	2.35	0.10	1.70	0.01
	15–20	2.44	0.15	1.74	0.02
	45–50	2.44	0.92	0.97	0.63
	95–100	4.19	1.59	0.31	0.29
Arable, AR1	0–5	2.54	0.06	2.01	0.05
	5–10	2.55	0.04	1.98	0.05
	15–20	2.16	0.35	2.05	0.05
	45–50	2.87	0.54	0.59	0.13
	95–100	9.49	2.83	0.03	0.01
Depth	RG1	NS		*	
	AR1	**		***	
Fertilisation	RG1	NS		NS	
	AR1	NS		NS	

There were no significant effects of fertiliser application, and the numbers shown are averaged across fertiliser treatments (n = 2)

*$p < 0.05$; **$p > 0.01$; ***$p < 0.001$

Table 2 The isotopic signatures of N$_2$O emitted from arable organic soil with potatoes in the cropping season 2015 were compared between eight individual periods that include spring and autumn periods. Differences between periods ($p < 0.05$) are indicated by different letters within a column

DOY	AR1 − F			AR1 + F		
	n	δ^{15}N$_{bulk}$ ‰	SP ‰	n	δ^{15}N$_{bulk}$ ‰	SP ‰
92–102	44	8.0de	2.7a	56	10.0d	4.1b
102–112	27	5.8de	13.3bc	61	− 10.1c	18.6d
126–136	26	− 7.3c	16.8 cd	21	8.8d	15.2 cd
136–145	6	− 5.1cde	24.3d	7	− 13.0bc	14.0 cd
145–155	40	− 11.9c	19.4d	48	− 13.5c	11.6c
155–136	49	− 21.7b	10.7c	39	− 22.6ab	7.1bc
258–260	22	− 54.6a	5.2a	13	− 54.0a	− 4.1a
268–273	41	10.4e	1.8a	21	13.9d	2.9b

The δ^{15}N$_{bulk}$ and SP of N$_2$O were tested with the non-parametric Kruskal–Wallis analysis of variance followed by Dunn's multiple comparison test

During the autumn monitoring period, the NH$_4^+$ concentrations at site AR1 remained low, while there was a significant accumulation of NO$_x^-$, either from decomposition of peat or from decomposition of residues from the potato crop, which was sprayed to terminate growth in mid-August. This NO$_x^-$ pool was depleted during September and reached the background level by DOY271.

Nitrous oxide emissions and isotopic signatures

The values of δ^{15}N$_{bulk}$ and SP of N$_2$O observed in ambient air were, respectively, 5.9 ± 2.5 and $13.0 \pm 2.8‰$, which were lower and more variable than values previously reported by Yoshida and Toyoda (2000) for δ^{15}N$_{bulk}$ ($7.0 \pm 0.6‰$) and SP ($18.7 \pm 2.2‰$). Wolf et al. (2015), using laser spectrometry, reported ranges of − 4.6 to 6.6‰ for δ^{15}N$_{bulk}$, and 14.3 to 19.3‰ for SP, in air above intensively managed grassland, suggesting that concentrations in ambient air
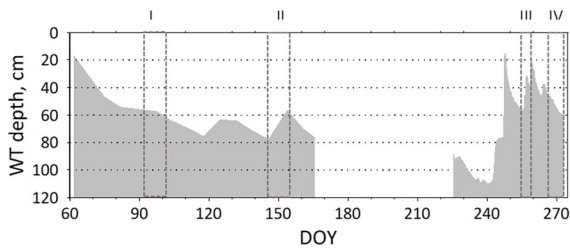
Fig. 4 Water table depth during the monitoring period; only weekly recordings were obtained during spring. Four periods are highlighted, i.e., I—DOY92-102; II—DOY145-155; III—DOY257-259; and IV—DOY268-273, for which monitoring results are presented in detail

can vary dynamically. There is still uncertainty associated with the experimental determination of isotope ratios of isotopocules of N_2O (Mohn et al. 2014), and since ambient concentrations of $\delta^{15}N^\alpha$ and $\delta^{15}N^\beta$ in N_2O were at the lower limit of detection for the laser instrument used in this study, approximate values of 7 and 18‰ were adopted for $\delta^{15}N_{bulk}$ and SP of ambient air in subsequent calculations (Toyoda et al. 2013; Harris et al. 2017).

Wolf et al. (2015) determined isotopic signatures using Keeling plots; high precision was achieved for a wide range of N_2O mixing ratios (lower limit: 12 ppb increase) by using a pre-concentration unit collecting N_2O from 8 l air, but fluxes were calculated for 24-h periods in order to obtain the N_2O concentration range needed for this approach. In the present study, measurements of fluxes and the associated isotopic

signatures were completed within 12 min, and since the isotopic signatures at low N_2O concentrations were unreliable (cf. Figure 3), we instead introduced a threshold of 600 ppb (i.e., ~ 275 ppb increase), above which the isotopic signatures stabilised. For this subset of data, the standard deviation of $\delta^{15}N_{bulk}$ and SP in the unfertilised subplot ($AR1 - F$; $n = 288$) were on average 2.2‰ (range 0.2–8.5‰) and 5.1‰ (range 0.4–20.4‰,). The corresponding values for $AR1 + F$ ($n = 298$) were 2.5‰ (range 0.4–8.5‰) for $\delta^{15}N_{bulk}$ of N_2O and 5.9‰ (range 1.2–17.0‰) for SP.
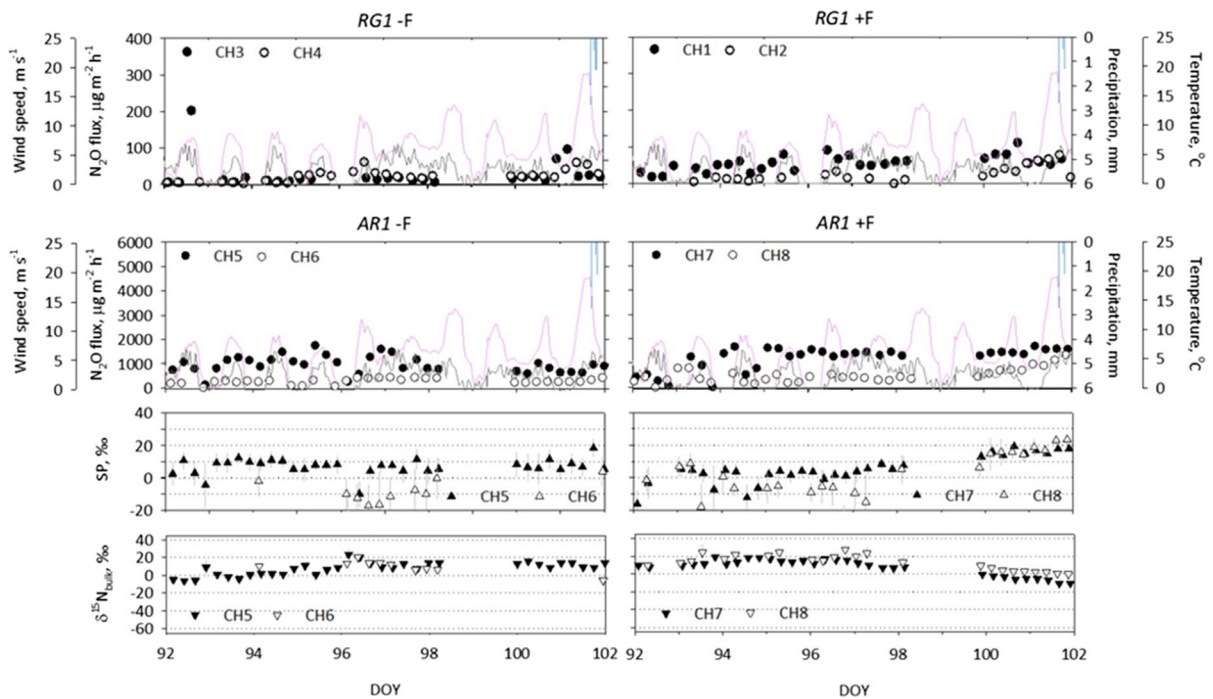
Period I (DOY92-102)

During early spring the $+ F$ and $-F$ subplots were effectively replicates, since N fertilisation did not take place until DOY106 ($RG1 + F$) or DOY141 ($AR1 + F$). Nitrous oxide emissions from the grassland treatments, $RG1 - F$ and $RG1 + F$, remained low at this time (Fig. 6, note different scales). At site $AR1$, as well as in treatment $RG1 + F$, the N_2O emissions were higher in block 2 compared to block 3 (Fig. 6, black symbols). The WT was 10–15 cm lower in block 2 at the upper slope position, and this could have resulted in a greater potential for N_2O formation and/ or transport through the soil.

The isotopic signatures showed a high degree of time series consistency. The SP of emitted N_2O varied
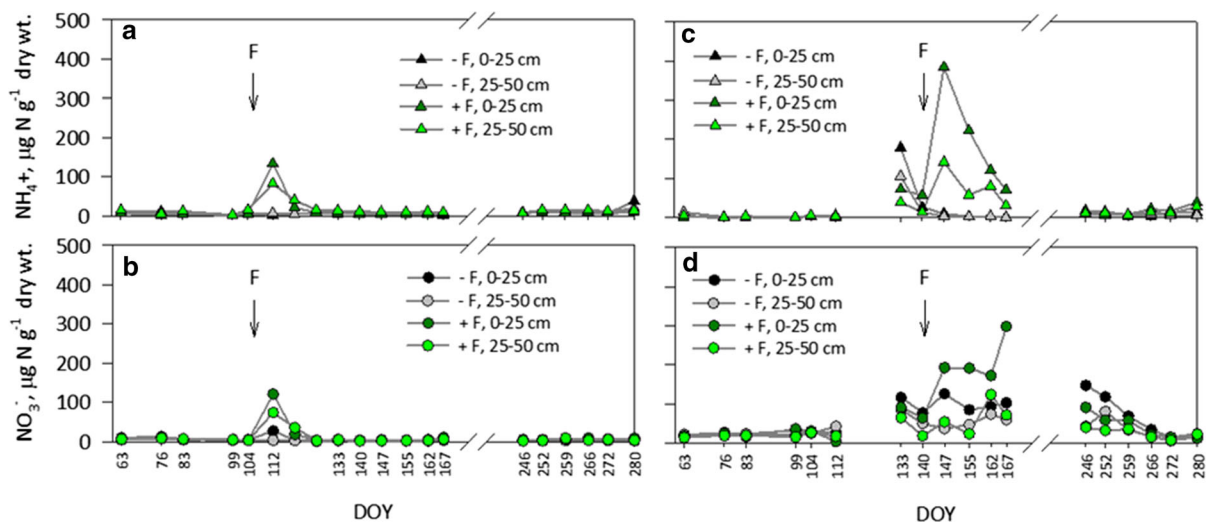
Fig. 5 Average concentrations of NH_4^+ in (**a**) treatment $RG1$ and (**c**) treatment $AR1$, as well as average concentrations of NO_x^- in (**b**) treatment $RG1$ and (**d**) treatment $AR1$, with ($+ F$)

and without ($- F$) fertilisation. Nitrogen fertilisation on DOY106 (RG1) and DOY141 (AR1) is indicated by "F"

Fig. 6 Nitrous oxide emissions from rotational grass (site *RG1*, top panel) and an adjacent arable field (site *AR1*, 2nd panel) in early spring (DOY92-102; Period I); note different scale. Also shown are precipitation (blue bars), air temperature (red line) and wind speed (grey line). The two lower panels show site preference (SP) and $\delta^{15}N_{bulk}$ at site *AR1* (see text)

between 0 and + 10‰ during DOY92-98, with some observations in block 3 as low as − 10‰, though uncertain. Meanwhile the $\delta^{15}N_{bulk}$ of N_2O varied between 0 and + 20‰. Minor diel variations in the isotopic signature of N_2O, especially for SP, seemed to align with the variation in N_2O flux. During DOY100-102, there was an increasing trend in SP towards + 20‰, and a corresponding decline for $\delta^{15}N_{bulk}$ of N_2O towards values at or below 0‰. Nitrous oxide emission rates were remarkably constant considering the variations in air temperature, indicating that N_2O was produced in a less fluctuating environment at depth in the soil.

Interestingly, there was a differentiation between CH5 and CH6 with respect to SP, but not $\delta^{15}N_{bulk}$ of N_2O (Fig. 6), suggesting a difference between Block 2 and 3 in the composition of sources and sinks, but not pathway of N_2O formation. There were no apparent increase in NH_4^+ or NO_3^- availability during this period (Fig. 5), but WT differed between the upper slope position (CH5, CH7) compared to the lower position (CH6, CH8), and both declined (Fig. 4). The

possible effects of WT dynamics on the isotopic composition of N_2O will be discussed later.

The trends described above were maintained during DOY102-112, with SP values in the range of + 10 to + 25‰ and $\delta^{15}N_{bulk}$ of N_2O in the range of from 0 to − 20‰ (Fig. S4), and during DOY 126-136 (Fig. S5) where, however, the higher emissions of N_2O now occurred at the lower slope position and few isotopic signatures were available for the upper slope position.

Period II (DOY145-155)

Nitrous oxide emissions from the grassland site remained low in late spring, although enhanced fluxes were seen in connection with rain events (Fig. 7, top panel). In the subplot without fertiliser (*RG1 − F*), N_2O was released only at the lower slope position (CH6), and only at the first rain event around DOY150. In the fertilised subplot, *RG1 + F*, N_2O emissions were enhanced after each of the three rain events. Soil mineral N was low at all three rain events (Fig. 5), which indicates that N_2O may have been induced by mineralisation of labile organic N, possibly
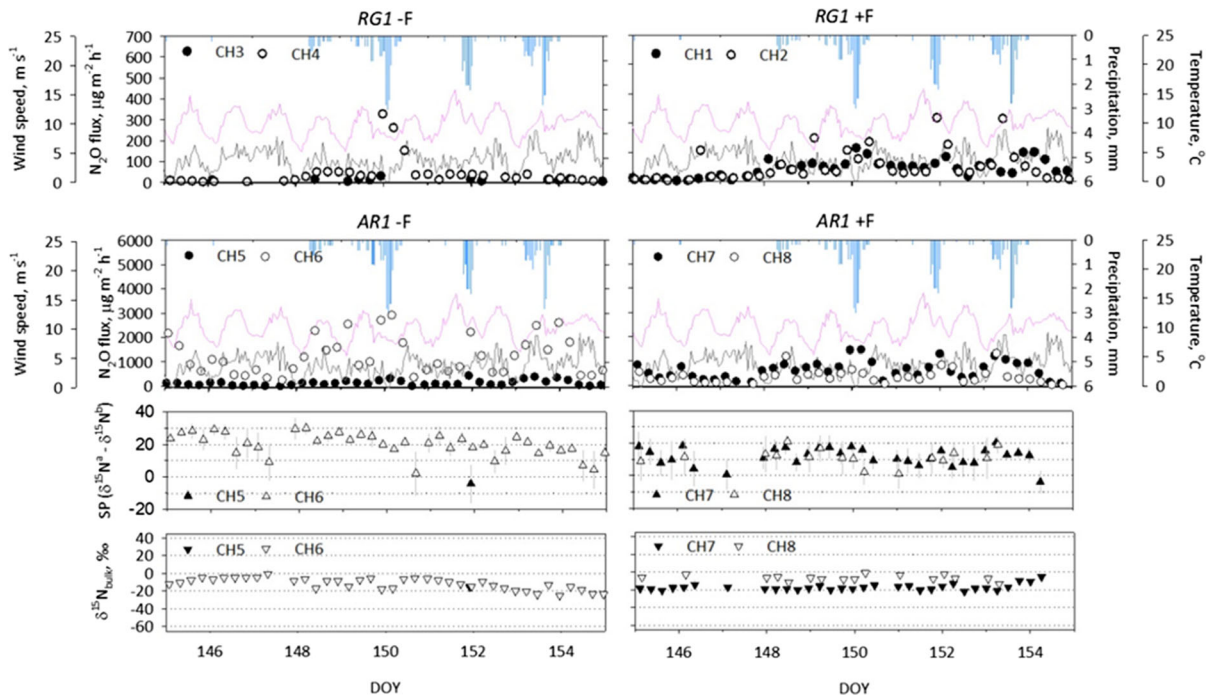
Fig. 7 Nitrous oxide emissions from rotational grass (site *RG1*, top panel) and an adjacent arable field (site *AR1*, 2nd panel) in late spring (DOY145-155; Period II); note different scale. Also shown are precipitation (blue bars), air temperature (red line) and wind speed (grey line). The two lower panels show site preference (SP) and $\delta^{15}N_{bulk}$ at site *AR1* (see text). (Color figure online)

as a result of rapid up-shifts in soil water potential following rain (Xu et al. 2004), as indicated by the detailed information about WT depth in the autumn (Fig. 4).

The N_2O emissions from site *AR1* were up to an order of magnitude higher compared to *RG1* despite a distance of only 10 to 20 m, and there was a consistent positive response to rain events. Notably, the N_2O emissions from block 2 (CH5 and CH7) had declined compared to Period I, whereas emissions from block 3 (especially from CH6) were now high (Fig. 7).

Fertilisation took place on DOY141, and on DOY146 the concentrations of NH_4^+–N and NO_x^-–N at 0–25 cm depth were, respectively, 384 and 193 mg kg^{-1} dry wt. soil in treatment *AR1 + F*, while the corresponding concentrations in treatment *AR1 − F* were 10 and 126 mg N kg^{-1} (Fig. 5). However, the cumulative N_2O emissions of treatment *AR1 + F* were similar to those of treatment *AR1 − F* (Taghizadeh-Toosi et al. 2019), and SP and $\delta^{15}N_{bulk}$ of N_2O were comparable or slightly lower in treatment *AR1 + F*. The fact that the overall

highest fluxes were seen at CH6 in the unfertilised treatment (*AR1 − F*) shows that soil properties were more important than fertilisation for N_2O emissions at this time.

Due to low N_2O emission rates, few isotope results were available for CH5 in this period. At CH6, the SP initially fluctuated between + 20 and + 30‰, declining after rainfall and thereby suggesting a shift in pathways of N_2O formation (Fig. 7). The $\delta^{15}N_{bulk}$ of N_2O in treatment *AR1 − F* showed little response to N_2O emission dynamics. There was a gradual shift from − 20‰ towards 0‰, which in treatment *AR1 − F* was reversed around DOY150.

Period III (DOY257-260)

For most of this period, N_2O emissions were measured only at site *AR1*, and a 3-h cycle could therefore be adopted. The period had frequent rainfall and a 35 cm rise in WT (Fig. 4). There was no immediate N_2O emission in response to 10 mm of rainfall during the night of DOY257 or, the following day, to 30 mm rain

within a 6-h period. Then, however, followed a period with enhanced N_2O emissions that were, as above, higher in treatment $AR1 − F$ compared to $AR1 + F$. Presumably the source of N_2O was NO_x^-, the concentration of which declined (Fig. 5c, d). This was supported by a graphical model analysis of N_2O emissions in a parallel study based on manual chamber measurements (Taghizadeh-Toosi et al. 2019). A flush of N_2O emissions after harvest of a potato crop was also observed in studies by Regina et al. (2004) and van Groenigen et al. (2005). The N_2O emissions were clearly higher from CH5 and CH7 at the upper slope position, suggesting again that gas transport was important in controlling emissions. Nitrous oxide emissions dropped abruptly following 8.4 mm rain during the evening of DOY259. It is not clear if saturation of the soil shifted the $N_2O:N_2$ product ratio towards N_2, or if soil wetness merely delayed soil-air gas exchange. There were no changes in the isotopic signature of N_2O that would suggest a major shift in source composition or pathways at this time. The SP stabilised around $+ 10‰$, while the $δ^{15}N_{bulk}$ values for N_2O were in the range of $− 40$ to $− 60‰$.

Period IV (DOY267-273)

This period had little rainfall, but pronounced diel variation in temperature and calm conditions during night (Fig. 8). At both sites an inverse relationship was indicated between N_2O emissions and temperature, i.e., the highest fluxes were observed when both temperature and wind speed were low or declining. A similar pattern had been suggested during the period DOY145-155 (Fig. 7). In the absence of wind to remove N_2O accumulating in air at the soil surface, N_2O will also accumulate in the soil below. If headspace mixing then reduced the diffusive boundary layer during flux measurements, this could have increased the N_2O concentration gradient between soil and air, enhancing gas exchange and the observed N_2O emission rates, as discussed by Korkiakoski et al. (2017).

During this period, the SP of N_2O fluctuated between 0 and $+ 10‰$, although some values were at $− 10‰$ or even lower. The $δ^{15}N_{bulk}$ of N_2O in treatment $AR1 − F$ were at $− 20$ to $0‰$ around DOY268, but then followed a rapid increase to between $+ 10$ and $+ 20‰$ by DOY269, followed by a gradual decline.

Sources of N_2O emissions

The seasonal dynamics with respect to rate and isotopic composition of N_2O indicated that sources and pathways of N_2O emissions from this acid organic soil varied across the year. The spatial and temporal patterns in N_2O emissions were related to WT depth and weather conditions, whereas effects of soil nitrogen status were complex. In period I, the soil contained little mineral N, and thus N_2O was probably derived from soil organic pools. Periods II and III were characterised by repeated rainfall and fluctuating WT (Fig. 4), and irrespective of N fertilisation there was a net accumulation of NO_x^- at site $AR1$, but not $RG1$ with active plant growth; this NO_x^- was probably derived from peat decomposition following WT drawdown or, in the autumn, decomposition of potato crop residues (Fig. 5). The soil NO_x^- pool was depleted during period IV.

A parallel study was conducted at the experimental site, in which N_2O emissions were monitored by weekly sampling in all three experimental blocks using manual chambers (Taghizadeh-Toosi et al. 2019). Using a generalised linear mixed model, it was shown that there was no effect of fertiliser N on N_2O emissions in neither $RG1$ nor $AR1$, which is evidence that N_2O was derived mainly from soil N pools. Previous studies of managed peatland found a high potential for denitrification, and that denitrifier activity was constrained by WT depth and N availability, rather than electron donors (Davidsson et al. 2002; van Beek et al. 2004; Palmer et al. 2016). Palmer et al. (2016) further showed that manipulating the WT of an acidic fen peat soil had only minor effects on denitrifier abundance or community composition. Nitrous oxide could be a main product of denitrification in acid soil due to impaired functionality of N_2O reductase (Baumann et al. 1997; Liu et al. 2014), and hence denitrification was a potential main source of N_2O emissions. The isotopic signatures of N_2O were used here to qualify this tentative conclusion.

As basis for discussing possible sources of N_2O, the mean values of SP and $δ^{15}N_{bulk}$ of N_2O were calculated for the individual periods and compiled in a scatter plot (Fig. 9), where the size of symbols indicates the magnitude of N_2O emissions in each period. Results include periods I to IV identified in Fig. 4, as well as observations in other periods not discussed in detail (Figs. S4 to S7). The standard
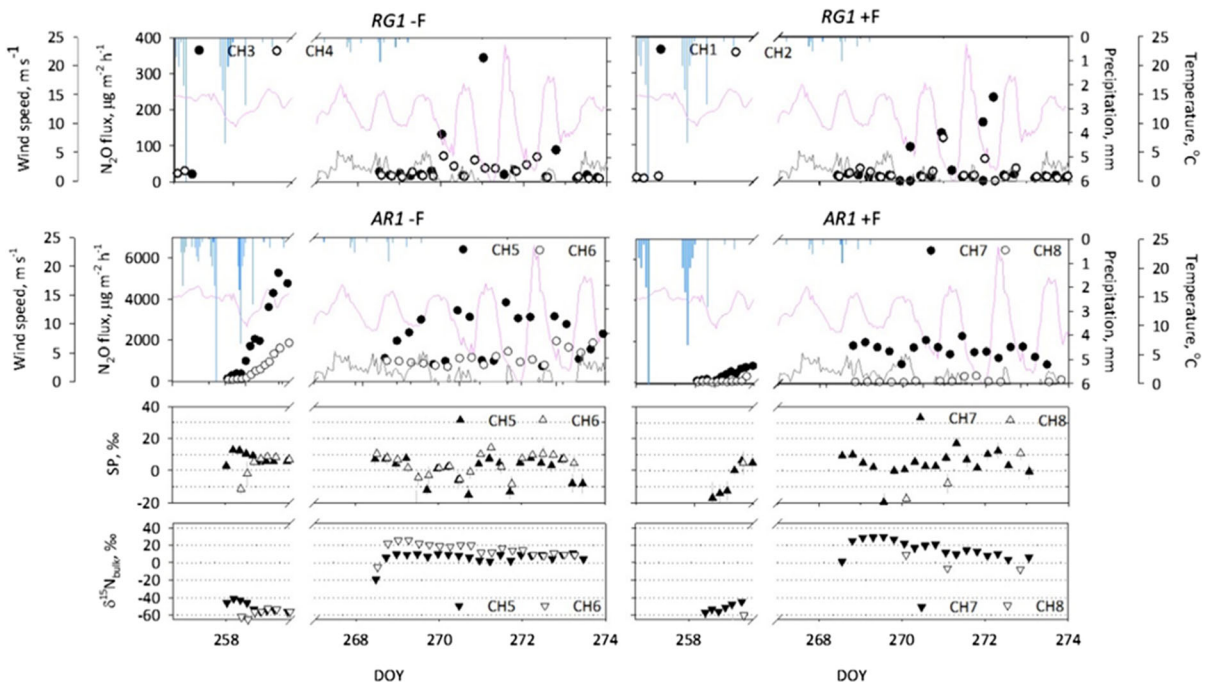
Fig. 8 Nitrous oxide emissions from rotational grass (site *RG1*, top panel) and an adjacent arable field (site *AR1*, 2nd panel) in autumn (DOY258-260; Period III and DOY268-273; Period IV); note different scale. Also shown are precipitation (blue bars), air temperature (red line) and wind speed (grey line). The two lower panels show site preference (SP) and $\delta^{15}N_{bulk}$ at site *AR1* (see text)
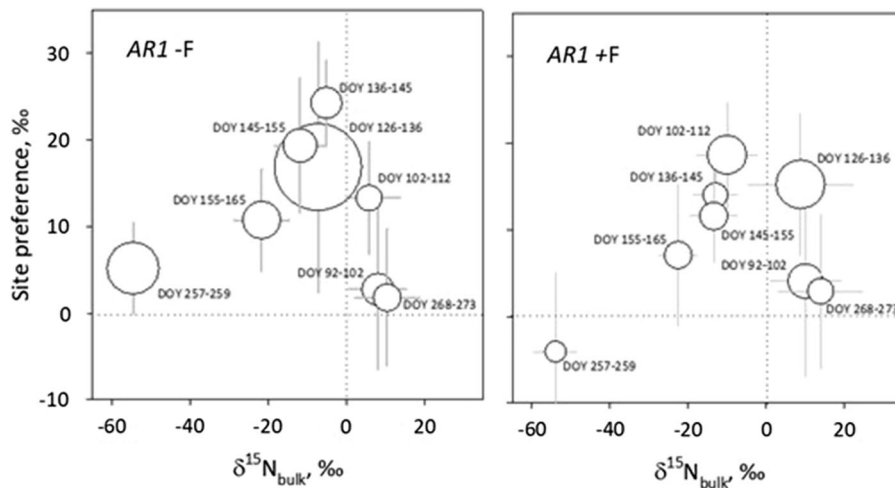
Fig. 9 The mean and standard deviation of SP and $\delta^{15}N_{bulk}$ of N_2O as observed in the eight individual periods indicated; standard deviations represent the within-period variations in N_2O isotopic composition. The magnitude of symbols is proportional to the average flux in the individual periods, as represented by the maximum concentration of N_2O during flux measurements

deviations shown represent the variation of observations within each period, and not the analytical errors of SP and $\delta^{15}N_{bulk}$ of N_2O, which were given above, but also in the caption of Fig. 9. Without knowledge about the ^{15}N enrichment of potential substrates, the mapping approach (e.g., Toyoda et al. 2017) could not

be used, and the results are discussed in this light. It should also be acknowledged that more robust data interpretation would have been possible by inclusion of ^{18}O–N_2O analyses, but this was not an option in this study. However, even this additional information will not fully resolve the relative importance of non-steady state reactions, substrate depletion, and N_2O reduction in situations, where substrate concentrations are unknown or below the method detection limit (Verhoeven et al. 2019).

While systematic differences in SP or $\delta^{15}N_{bulk}$ of N_2O between blocks (i.e., slope positions) were seen in several cases, the overall variation was dominated by temporal changes. The mean SP and $\delta^{15}N_{bulk}$ of N_2O observed in the first (I) and last (IV) measurement periods, referred to below as *shoulder seasons*, were remarkably close. In the intermediate *mid-season* periods, characterised by accumulation of mineral N from fertiliser input and net N mineralisation, there was a trend of increasing, and then decreasing SP, and a general decline in $\delta^{15}N_{bulk}$ of N_2O. In the following, shoulder seasons and mid-season period are discussed separately.

Shoulder season periods

The contents of NH_4^+ and NO_3^- were low in these periods with declining WT, and hence N_2O emissions probably depended on mineralisation and transformations of N following drainage of saturated layers. In accordance with this, Taghizadeh-Toosi et al. (2019) found that soil N_2O concentration above the WT depth was the main predictor of N_2O emissions during spring. The isotopic signatures of N_2O in the shoulder seasons were characterised by SP of + 2 to + 4‰ and an average $\delta^{15}N_{bulk}$ of N_2O of + 8 to + 14‰. Thus, SP values suggested that bacterial denitrification or nitrifier-denitrification were main pathways of N_2O, but positive $\delta^{15}N_{bulk}$ values were unexpected. Potential sources of N_2O (fertiliser, residues, peat) had $\delta^{15}N$ of 0 to + 5‰, and nitrification as well as denitrification show isotope effects of − 30 to − 15‰ or more in pure culture studies (Denk et al. 2017). Well-decomposed peat is dominated by dead-end pores having a slow exchange of solutes with active pore volumes (Hoag and Price 1997), and substrate limitation at the cellular level would reduce the potential for isotope discrimination during N transformation processes

(Casciotti et al. 2011), but this does not account for $\delta^{15}N_{bulk}$ of N_2O above the values of potential substrates. A potential mechanism is N_2O reduction to N_2, which has been demonstrated in a variety of environments (Clough et al. 2005; Ostrom et al. 2007; Mothet et al. 2013; Yano et al. 2014). The possible role of N_2O reduction is discussed below.

With decomposing peat as a main source of N_2O in shoulder seasons, ammonia oxidation would have to be involved in N_2O formation. Ammonia oxidising archaea were expected to dominate ammonia oxidation at the low pH of this soil because of their much higher affinity for NH_3 compared to AOB (Prosser and Nicol 2012). For example, He et al. (2012) cited K_m values of 0.0023 to 0.04 μM for AOA, and 3 to 26 μM for AOB isolated from soil. Jung et al. (2014) reported SP values of N_2O produced by five AOA of + 20 to + 30‰, and $\delta^{15}N_{bulk}$ values of − 17 to − 13‰, and hence ammonia oxidation alone was probably not a direct source of N_2O in shoulder seasons. However, nitrifier activity could still be an indirect driver of N_2O emissions.

In late April, the acid peat at site *AR1* contained up to 10 mg NO_2^-–N in the capillary fringe (Taghizadeh-Toosi et al. 2019), confirming ammonia oxidation activity. Nitrifier denitrification to remove toxic levels of HNO_2 in this acid environment could be a mechanism to explain N_2O formation (Poth and Focht 1985). On the other hand, the acid peat also contained 5 mg kg^{-1} total reactive iron (TRFe) in the capillary fringe (Taghizadeh-Toosi et al. 2019), and hence chemodenitrification could be an abiotic pathway to N_2O formation, especially since chemodenitrification is stimulated by increasing concentrations of Fe^{2+} and declining pH (van Cleemput and Samater 1996). The range of $\delta^{15}N_{bulk}$ of N_2O reported by Buchwald et al. (2016) for chemodenitrification in batch incubation experiments was − 20 to − 3‰, and the SP values were + 15 to + 26‰ for SP, which were not consistent with the composition of N_2O emitted in shoulder seasons. It should be noted, however, that Buchwald et al. (2016) also found SP values close to 0‰ under Fe^{2+} limiting conditions, which are not incompatible with high bulk soil concentrations. Estop-Aragonés et al. (2012) showed that transition zones between oxic and anoxic conditions in peat soil occur in the capillary fringe, and hence NO_2^- and Fe^{2+} accumulating in oxic and anoxic sites,

respectively, may have reacted around oxic-anoxic interfaces.

Mid-season periods

There were some differences between isotopic signatures with and without N fertiliser in individual periods, but this occurred before, as well as after fertilisation took place, and therefore both treatments are discussed together. In mid-season monitoring periods, the SP values were in the range of + 15 to + 25‰ until DOY155 and then declined to around + 10‰ by mid-June (DOY155-165), while $\delta^{15}N_{bulk}$ of N_2O showed a declining trend to − 20‰ by this time. The SP values of + 15 to + 25‰ would be consistent with ammonia oxidation and/or fungal denitrification as the main pathway to N_2O emissions. Fungal denitrification has been associated with high N_2O emissions from acid soil (Yanai et al. 2007; Rütting et al. 2013; Huang et al. 2017). Rütting et al. (2013) discussed possible associations between fungi and bacterial denitrifiers in an organic forest soil and concluded that the relative importance of fungal and bacterial denitrification in acid soil is not readily resolved. Rohe et al. (2014) found, for N_2O production by six fungal denitrifiers, that N isotope effects ranged from − 18 to − 9‰ and SP values from + 22 to + 36‰, with NO_2^- as electron acceptor, and hence this process could have been a sink for NO_2^- produced via nitrification. Interestingly, a recent paper investigating chemodenitrification from reaction of NO_2^- with a range of organic sources, including soils, found SP values in the range of + 20 to + 30‰, and $\delta^{15}N_{bulk}$ of N_2O of around − 40‰ (Wei et al. 2019). Chemodenitrification was discussed by Taghizadeh-Toosi et al. (2019) as a possible source of N_2O during spring in the arable soil investigated here.

The $\delta^{15}N_{bulk}$ of N_2O were lower compared to shoulder seasons. The declining WT was probably accompanied by increasing air-filled porosity in drained soil layers, and this may have reduced the potential for N_2O reduction during transport to the soil surface. High emissions of N_2O often occurred after rain events, which resulted in dynamic increases in WT depth and soil water content as judged from the short-term dynamics of WT recorded in the autumn period (Fig. 4). The main source at this time may have been the NO_x^- accumulating in the top soil (Fig. 5), which would involve a shorter transport distance and

hence lower potential for N_2O reduction. The isotopic signatures of N_2O in period III (DOY257-259) were more closely related to bacterial denitrification (Denk et al. 2017). These fluxes represent a period with excess NO_x^- and thus no substrate limitation for heterotrophic denitrification; the subsequent shift in isotopic signature to period IV (DOY268-273) was striking.

Nitrous oxide reduction

During shoulder seasons, $\delta^{15}N_{bulk}$ values were observed which clearly exceeded the $\delta^{15}N$ of the peat, as well as fertiliser N and potato crop residues. During September, soil NO_x^- concentrations at 0 to 25 cm depth declined from 91 to 15 mg N kg^{-1} in treatment *AR1 − F*, and from 147 to 15 mg N kg^{-1} in treatment *AR1 + F* (Fig. 5), and Taghizadeh-Toosi et al. (2019) concluded in a parallel study conducted at the site that denitrification was the main source of N_2O at site *AR1* in this period. It is therefore relevant to consider if increases in $\delta^{15}N_{bulk}$ of N_2O through N_2O reduction (Toyoda et al. 2017) could account for the observations assuming N_2O was produced mainly via denitrification of NO_x^-. As already mentioned, an important limitation in the present study is the lack of information about the enrichment of NO_x^-. Koba et al. (2009) reported $\delta^{15}N$ of NO_3^- in the range of − 2.1 to + 6.6‰ in groundwater under a forest. Verhoeven et al. (2019; see Fig. S9) determined $\delta^{15}N$ of NO_3^- in pore water extracted from surface soil of a rice field and found most values at 5 and 12.5 cm depth within approximately ± 5‰ except for a period after flooding, where values increased. This information may qualify the assumption chosen for the calculations below that the enrichment of NO_x^- was ∼ 0‰.

The extent of N_2O reduction was estimated using the equations for a Rayleigh distillation process described by Mariotti et al. (1981), i.e.,:

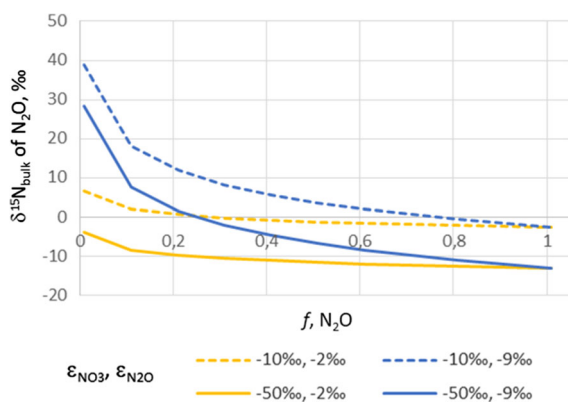$$\delta_s(t) = \delta_s(t_0) + \varepsilon_{p/s} lnf \qquad (6)$$

where δ_s represents the ^{15}N enrichment of NO_x^- at time t and t_0, respectively, $\varepsilon_{p/s}$ is the enrichment factor for NO_x^- reduction to N_2O, and f is the proportion of remaining substrate (here: NO_x^-) at time t. The ^{15}N enrichment of the product, N_2O, would change according to:

$$\delta_p(t) = \delta_s(t_0) - \varepsilon_{p/s} \frac{f\ln(f)}{(1-f)} \quad (7)$$

where δ_p is the ^{15}N enrichment of N_2O produced by NO_x^- reduction, and identical to δ_s for N_2O reduction. In a review by Park et al. (2011), soil enrichment (ε) factors for NO_3^- reduction to N_2O ranged from -50 to $-10‰$, while ε values for N_2O reduction to N_2 ranged from -9 to $-2‰$. These ranges are largely consistent with results reviewed by Denk et al. (2017). Based on the proportion of NO_x^- removed in treatment $AR1 + F$ (90%), and the ε ranges given above as lower and upper boundaries, the theoretical $\delta^{15}N_{bulk}$ of N_2O would be -13 to $-2.6‰$ in the absence of N_2O reduction, and -3.8 to $+38.9‰$ with N_2O reduction varying between 1 and 99% (Fig. 10). According to this calculation, 80 to 90% removal by N_2O reduction would be required to account for the highest $\delta^{15}N_{bulk}$ values of $+8$ to $+14‰$ observed. Buchen et al. (2016) estimated N_2O reduction of 90% in an organic soil, suggesting that such reduction can occur. Also, Menyailo and Hungate (2006) found, in batch incubation experiments to study N_2O reduction, enrichments of $\delta^{15}N_{bulk}$ of N_2O up to $+13$ to $+17‰$ when N_2O was nearly depleted. On the other hand, these calculations were based on a closed system, which may overestimate the extent of N_2O reduction (Wu et al. 2016).

While reduction of N_2O produced via denitrification thus could explain the $\delta^{15}N_{bulk}$ of N_2O observed, it should be reiterated that observations could also be partly accounted for by isotope effects related to soil NO_x^-. In addition to the field observations of Koba et al. (2009) and Verhoeven et al. (2019) cited above, an inverse isotope effect during NO_2^- oxidation has been reported in pure culture studies, in which $\delta^{15}N$ of NO_3^-–N changed by $+13‰$ (Denk et al. 2017). Bergstermann et al. (2011) also observed a change in $\delta^{15}N_{bulk}$ of added NO_3^- from 0 to $+20‰$ within 4 days of batch incubation, and a corresponding shift in the enrichment of N_2O. Additional information about the ^{15}N enrichment of mineral N pools and N_2O in the soil profile may be necessary to determine the relative importance of N_2O reduction, but it is complicated by the difficulties of obtaining such information at the scale relevant for biogeochemical transformations (Koba et al. 2009), and at low soil mineral N availabilities (Verhoeven et al. 2019).

Conclusion

Emissions of N_2O from adjacent sites on acid organic soil with either rotational grass or a potato crop were up to 400 and 6000 µg m^{-2} h^{-1} and highly variable, as hypothesized. The N_2O emissions were strongly related to WT dynamics and individual rain events, slope position and soil mineral N availability. Isotopic signatures could be obtained with static chamber measurements provided there was a *c.* twofold increase in headspace N_2O concentration. Isotopic signatures of N_2O emitted from the arable site indicated a shift in source composition between shoulder seasons with N limitation and declining WT depth, and mid-season periods with mineral N accumulation in the soil. Diel variation in SP or $\delta^{15}N_{bulk}$ of N_2O were not evident at the resolution achieved in this study, which indicated that the source of N_2O within individual periods was well-defined. The relative importance of N_2O production pathways could not be resolved on the basis of SP and $\delta^{15}N_{bulk}$ of N_2O alone, partly because of the unknown, but probably in some periods extensive N_2O reduction within microsites or during transport to the soil surface, and partly because the enrichment of substrates was unknown. Depending on the importance of N_2O reduction and isotope effects due to substrate limitation, the composition of N_2O emitted could be explained by a combination of several denitrification processes, i.e., bacterial denitrification, nitrifier

Fig. 10 A theoretical calculation of the enrichment of $\delta^{15}N_{bulk}$ of N_2O under different scenarios regarding enrichment during NO_3^- reduction to N_2O (boundaries -50 and $-10‰$), and during N_2O reduction to N_2 (boundaries -9 to $-2‰$); ranges for processes in soil as reported by Park et al. (2011)

denitrification, chemodenitrification and fungal denitrification, and with an unknown contribution from ammonia oxidation during mid-season periods. The relative importance of individual sources and pathways changed during the year, and thus site-specific information about soil conditions, isotopic composition of potential N_2O precursor molecules, and information about microbial community composition and activity, will be needed for correct interpretation of isotopic signatures.

References

Aerts R, Ludwig F (1997) Water-table changes and nutritional status affect trace gas emissions from laboratory columns of peatland soils. Soil Biol Biochem 29:1691–1698

Andert J, Börjesson G, Hallin S (2011) Temporal changes in methane oxidizing and denitrifying communities and their activities in a drained peat soil. Wetlands 32:1047–1055

Baumann B, van der Meer JR, Snozzi M, Zehnder AJB (1997) Inhibition of denitrification activity but not of mRNA induction in Paracoccus denitrificans by nitrite at a suboptimal pH. Antonie Van Leeuwenhoek 72:183–189

Bergstermann A, Cardenas L, Bol R, Gilliam L, Goulding K, Meijide A, Scholefield D, Vallejo A, Well R (2011) Effect of antecedent soil moisture conditions on emissions and isotopologue distribution of N_2O during denitrification. Soil Biol Biochem 43:240–250

Broder T, Blodau C, Biester H, Knorr KH (2012) Peat decomposition records in three pristine ombrotrophic bogs in southern Patagonia. Biogeosci 9:1479–1491

Buchen C, Lewicka-Szczebak D, Fuß R, Helfrich M, Flessa H, Well R (2016) Fluxes of N_2 and N_2O and contributing processes in summer after grassland renewal and grassland conversion to maize cropping on a Plaggic Anthrosol and a Histic Gleysol. Soil Biol Biochem 101:9–16

Buchwald C, Grabb K, Hansel CM, Wankel SD (2016) Constraining the role of iron in environmental nitrogen transformations: dual stable isotope systematics of abiotic NO_2 reduction by Fe(II) and its production of N_2O. Geochim Cosmochim Acta 186:1–12

Camin F, Moschella A, Miselli F, Parisi B, Versini G, Ranalli P et al (2007) Evaluation of markers for the traceability of potato tubers grown in an organic versus conventional regime. J Sci Food Agric 87:1330–1336

Casciotti KL, Buchwald C, Santoro AE, Frame C (2011) Assessment of nitrogen and oxygen isotopic fractionation during nitrification and its expression in the marine environment. Meth Enzymol 486:253–280

Clough TJ, Sherlock RR, Rolston DE (2005) A review of the movement and fate of N_2O in the subsoil. Nutr Cycl Agroecosyst 72:3–11

Davidsson TE, Trepel M, Schrautzer J (2002) Denitrification in drained and rewetted minerotrophic peat soils in Northern Germany (Pohnsdorfer Stauung). J Plant Nutr Soil Sci 165:199–204

Denk TRA, Mohn J, Decock C, Lewicka-Szczebak D, Harris E, Butterbach-Bahl K, Kiese R, Wolf B (2017) The nitrogen cycle: a review of isotope effects and isotope modeling approaches. Soil Biol Biochem 105:121–137

Erler DV, Duncan TM, Murray R, Maher DT, Santos IR, Gatland JR, Mangion P, Eyre BD (2015) Applying cavity ring-down spectroscopy for the measurement of dissolved nitrous oxide concentrations and bulk nitrogen isotopic composition in aquatic systems: correcting for interferences and field application. Limnol Ocenaogr 13:391–401

Estop-Aragonés C, Knorr K-H, Blodau C (2012) Controls on in situ oxygen and dissolved inorganic carbon dynamics in peats of a temperate fen. J Geophys Res 117:G02002

Goldberg SD, Knorr K-H, Blodau C, Lischeid G, Gebauer G (2010) Impact of altering the water table height of an acidic fen on N_2O and NO fluxes and soil concentrations. Glob Change Biol 16:220–233

Görres C-M, Conrad R, Petersen SO (2013) Effect of soil properties and hydrology on Archaeal community composition in three temperate grasslands on peat. FEMS Microbiol Ecol 85:227–240

Gregory AS, Dungait JAJ, Watts CW, Bol R, Dixon ER, White RP, Whitmore AP (2016) Long-term management changes topsoil and subsoil organic carbon and nitrogen dynamics in a temperate agricultural system. Eur J Soil Sci 67:421–430

Harris E, Henne S, Hüglin C, Zellweger C, Tuzson B, Ibraim E, Emmenegger L, Mohn J (2017) Tracking nitrous oxide emission processes at a suburban site with semicontinuous, in situ measurements of isotopic composition. J Geophys Res Atmos 122:1850–1870

He JZ, Hu HW, Zhang LM (2012) Current insights into the autotrophic thaumarchaeal ammonia oxidation in acidic soils. Soil Biol Biochem 55:146–154

Herrmann M, Hädrich A, Küsel K (2012) Predominance of thaumarchaeal ammonia oxidizerabundance and transcriptional activity in an acidic fen. Environ Microbiol 14:3013–3025

Hoag RS, Price JS (1997) The effects of matrix diffusion on solute transport and retardation in undisturbed peatin laboratory columns. J Contam Hydrol 28:193–205

Hu H-W, Chen D, He J-Z (2015) Microbial regulation of terrestrial nitrous oxide formation: understanding the biological pathways for prediction of emission rates. FEMS Microbiol Rev 39:729–749

Huang Y, Xiao X, Long X (2017) Fungal denitrification contributes significantly to N_2O production in a highly acidic tea soil. J Soils Sedim 17:1599–1606

IPCC (2014) 2013 Supplement to the 2006 IPCC guidelines for national greenhouse gas inventories. In: Hiraishi T, Krug T, Tanabe K, Srivastava N, Baasansuren J, Fukuda M, Troxler TG (eds) Wetlands. IPCC, Switzerland

Jung M-Y, Well R, Min D, Giesemann A, Park S-J, Kim JG, Kim S-J, Rhee S-K (2014) Isotopic signatures of N_2O produced by ammonia-oxidizing archaea from soils. ISME J 8:1115–1125

Koba K, Osaka K, Tobari Y, Toyoda S, Ohte N, Katsuyama M et al (2009) Biogeochemistry of nitrous oxide in groundwater in a forested ecosystem elucidated by nitrous oxide isotopomer measurements. Geochim Cosmochim Acta 73:3115–3133

Korkiakoski M, Tuovinen J-P, Aurela M, Koskinen M, Minkkinen K, Ojanen P, Penttilä T, Rainne J, Laurila T, Lohila A (2017) Methane exchange at the peatland forest floor—automatic chamber system exposes the dynamics of small fluxes. Biogeosciences 14:1947–1967

Leppelt T, Dechow R, Gebbert S, Freibauer A, Lohila A, Augustin J, Drösler M, Fiedler S, Glatzel S, Höper H, Järveoja J, Lærke PE, Maljanen M, Mander Ü, Mäkiranta P, Minkkinen K, Ojanen P, Regina K, Strömgren M (2014) Nitrous oxide emission budgets and land-use-driven hotspots for organic soils in Europe. Biogeosciences 11:6595–6612

LI-COR (2014) Capturing and processing soil GHG fluxes using the LI-8100A. LI-8100A Technical application note No 138, p 8

Liu B, Frostegård Å, Bakken LR (2014) Impaired reduction of N_2O to N_2 in acid soils is due to a posttranscriptional interference with the expression of nosZ. MBio 5:e01383

Madsen HB, Jensen NH (1988) Potentially acid sulfate soils in relation to landforms and geology. CATENA 15:137–145

Madsen HB, Rønsbo J, Holst MK (2000) Comparison of the composition of iron pans in Danish burial mounds with bog iron and spodic material. CATENA 39:1–9

Mander Ü, Uuemaa E, Kull A, Kanal A, Maddison M, Soosaar K, Salm J-O, Lesta M, Hansen R, Kuller R, Harding A, Augustin J (2010) Assessment of methane and nitrous oxide fluxes in rural landscapes. Landsc Urban Plan 98:172–181

Mariotti A, Germon JC, Hubert P, Kaiser P, Letolle R, Tardieu A, Tardieux P (1981) Experimental determination of nitrogen kinetic isotopic fractionation: some principles; illustration for the denitrification and nitrification processes. Plant Soil 62:413–430

Menyailo OV, Hungate BA (2006) Stable isotope discrimination during soil denitrification: production and consumption of nitrous oxide. Global Biogeochem Cycl 20:GB3025

Mohn J, Guggenheim C, Tuzson B, Vollmer MK, Toyoda S, Yoshida N, Emmenegger L (2010) A liquid nitrogen-free preconcentration unit for measurements of ambient N_2O isotopomers by QCLAS. Atmos Meas Tech 3:609–618

Mohn J, Tuzson B, Manninen A, Yoshida N, Toyoda S, Brand WA, Emmenegger L (2012) Site selective real-time measurements of atmospheric N_2O isotopomers by laser spectroscopy. Atmos Meas Tech 5:1601–1609

Mohn J, Wolf B, Toyoda S, Lin C-T, Liang M-C, Brüggemann N et al (2014) Interlaboratory assessment of nitrous oxide isotopomer analysis by isotope ratio mass spectrometry and laser spectroscopy: current status and perspectives. Rapid Commun Mass Spectrom 28:1995–2007

Mothet A, Sebilo M, Laverman AM, Vaury V, Mariotti A (2013) Is site preference of N_2O a tool to identify benthic denitrifier N_2O? Environ Chem 10:281–284

Nguyen QV, Wu D, Kong XW, Bol R, Petersen SO, Jensen LS, Liu S, Brüggemann N, Glud RN, Larsen M, Bruun S (2017) Effects of cattle slurry and nitrification inhibitor application on spatial soil O_2 dynamics and N_2O production pathways. Soil Biol Biochem 114:200–209

Nishida M, Sato Y (2015) Characteristics of the relationship between natural ^{15}N abundances in organic rice and soil. Plant Prod Sci 18:180–186

Ostrom NE, Pitt AJ, Sutka RL, Ostrom PH, Grandy AS, Huizinga KM, Robertson GP (2007) Isotopologue effects during N_2O reduction in soils and in pure cultures of denitrifiers. J Geophys Res Biogeosci 112:G02005

Palmer K, Köpp J, Gebauer G, Horn MA (2016) Drying-rewetting and flooding impact denitrifier activity rather than community structure in a moderately acidic fen. Front Microbiol 7:727

Park S, Pérez T, Boering K, Trumbore S, Gil J, Marquina S, Tyler S (2011) Can N_2O stable isotopes and isotopomers be useful tools to characterize sources and microbial pathways of N_2O production and consumption in tropical soils? Global Biogeochem Cycl 25:GB1001

Pedersen AR, Petersen SO, Schelde K (2010) A comprehensive approach to soil-atmosphere trace-gas flux estimation with static chambers. Eur J Soil Sci 61:888–902

Petersen SO, Hoffmann CC, Schäfer C-M, Blicher-Mathiesen G, Elsgaard L, Kristensen K, Larsen SE, Torp SB, Greve MH (2012) Annual emissions of CH_4 and N_2O, and ecosystem respiration, from eight organic soils in Western Denmark managed by agriculture. Biogeosciences 9:403–422

Poth M, Focht DD (1985) ^{15}N kinetic analysis of N_2O production by Nitrosomonas europaea—an examination of nitrifier denitrification. Appl Environ Microbiol 49:1134–1141

Prosser JI, Nicol GW (2012) Archaeal and bacterial ammonia oxidisers in soil: the quest for niche specialisation and differentiation. Trends Microbiol 20:523–531

R Core Team (2016) R: a language and environment for statistical computing. R Foundation for Statistical Computing. Vienna, Austria. https://www.R-project.org/

Regina K, Syväsalo E, Hannukkala A, Esala M (2004) Fluxes of N_2O from farmed peat soils in Finland. Eur J Soil Sci 55:591–599

Rohe L, Anderson T-H, Braker G, Flessa H, Giesemann A, Lewicka-Szczebak D, Wrage-Mönnig N, Well R (2014) Dual isotope and isotopomer signatures of nitrous oxide from fungal denitrification—a pure culture study. Rapid Commun Mass Spectrom 28:1893–1903

Rütting T, Huygens D, Boeckx P, Staelens J, Klemedtsson L (2013) Increased fungal dominance in N_2O emission hotspots along a natural pH gradient in organic forest soil. Biol Fertil Soils 49:715–721

Spott O, Russow R, Stange CF (2011) Formation of hybrid N_2O and hybrid N_2 due to codenitrification: first review of a barely considered process of microbially mediated N-nitrosation. Soil Biol Biochem 43:1995–2011

Stieglmeier M, Mooshammer M, Kitzler B, Wanek W, Zechmeister-Boltenstern S, Richter A, Schleper C (2014) Aerobic nitrous oxide production through N-nitrosating hybrid formation in ammonia-oxidizing archaea. ISME J 8:1135–1146

Sutka RL, Ostrom NE, Ostrom PH, Breznak JA, Gandhi H, Pitt AJ (2006) Distinguishing N_2O production from nitrification versus denitrification based on isotopomer abundances. Appl Environ Microbiol 72:638–644

Taghizadeh-Toosi A, Elsgaard L, Clough T, Labouriau R, Ernstsen V, Petersen SO (2019) Regulation of N_2O emissions from acid organic soil drained for agriculture. Biogeosciences 16:4555–4575. https://doi.org/10.5194/bg-2019-14

Toyoda S, Kuroki N, Yoshida N, Ishijima K, Tohjima Y, Machida T (2013) Decadal time series of tropospheric abundance of N_2O isotopomers and isotopologues in the Northern Hemisphere obtained by the long-term observation at Hateruma Island, Japan. J Geophys Res Atmos 118:3369–3381

Toyoda S, Yoshida N, Koba K (2017) Isotopocule analysis of biologically produced nitrous oxide in various environments. Mass Spectrom Rev 36:135–160

Van Beek CL, Hummelink EWJ, Velthof GL, Oenema O (2004) Denitrification rates in relation to groundwater level in a peat soil under grassland. Biol Fertil Soils 39:329–336

Van Cleemput O, Samater AH (1996) Nitrite in soils: accumulation and role in the formation of gaseous N compounds. Fertil Res 45:81–89

Van Groenigen JW, Zwart KB, Harris D, van Kessel C (2005) Vertical gradients of $\delta15$ N and $\delta18O$ in soil atmospheric N_2O—temporal dynamics in a sandy soil. Rapid Commun Mass Spectrom 19:1289–1295

Verhoeven E, Barthel M, Yu L, Celi L, Said-Pullicino D, Sleutel S, Lewicka-Scezcbak Six J, Decock C (2019) Early season N_2O emissions under variable water management in rice systems: source-partitioning emissions using isotope ratios along a depth profile. Biogeosciences 16:383–408

Wei J, Ibraim E, Brüggemann N, Vereecken H, Mohn J (2019) First real-time isotopic characterisation of N_2O from chemodenitrification. Geochim Cosmochim Acta 267:17–32

Well R, Kurganova I, De Gerenyu VL, Flessa H (2006) Isotopomer signatures of soil-emitted N_2O under different moisture conditions—a microcosm study with arable loess soil. Soil Biol Biochem 38:2923–2933

Wolf B, Merbold L, Decock C, Tuzson B, Harris E, Six J, Emmenegger L, Mohn J (2015) First on-line isotopic characterization of N_2O above intensively managed grassland. Biogeosciences 12:2517–2531

Wu D, Köster JR, Cardenas LM, Brüggemann N, Lewicka-Szczebak D, Bol R (2016) N_2O source partitioning in soils using 15 N site preference values corrected for the N_2O reduction effect. Rapid Commun Mass Spectrom 30:620–626

Xu L, Baldocchi DD, Tang J (2004) How soil moisture, rain pulses, and growth alter the response of ecosystem respiration to temperature. Global Biogeochem Cycl 18:GB4002

Yanai Y, Toyota K, Morishita T, Takakai F, Hatano R, Limin SH, Darung U, Dohong S (2007) Fungal N_2O production in an arable peat soil in Central Kalimantan, Indonesia. Soil Sci Plant Nutr 53:806–811

Yano M, Toyoda S, Tokida T, Hayashi K, Hasegawa T, Makabe A, Koba K, Yoshida N (2014) Isotopomer analysis of production, consumption and soil-to-atmosphere emission processes of N_2O at the beginning of paddy field irrigation. Soil Biol Biochem 70:66–78

Yoshida N, Toyoda S (2000) Constraining the atmospheric N_2O budget from intramolecular site preference in N_2O isotopomers. Nature 405:330–334